An experimental note on finite-amplitude standing gravity waves

By DAVE FULTZ

Hydrodynamics Laboratory, Department of the Geophysical Sciences, University of Chicago

(Received 19 January, 1962)

In a recent paper Tadjbakhsh & Keller (1960) have predicted that two-dimensional finite standing gravity waves in a rectangular container will have lower frequency than infinitesimal standing waves in deep water but have higher frequency below a certain mean depth to wavelength ratio. This is in strong contrast to the frequency results for finite progressive waves obtained by many investigators. Experimental confirmation of this prediction is reported together with estimates of the magnitude of the frequency effects at several depths. The frequency effect reversal appears to occur at a depth ratio of 0·14, somewhat less than the predicted ratio of 0·17.

Introduction

During the 1950's there has been a great revival of theoretical and experimental interest in surface gravity wave motions on the part of scientists in a number of different areas of investigation. Among these studies are a large number concerned with the class of standing gravity waves on bodies of liquid in fixed or moving containers (Cooper 1960). This class of fluid wave motions is among the earliest to have been thoroughly treated in the approximation of infinitesimal motions, e.g. by Merian (1828) for rectangular containers, and in the late nineteenth century was quite actively studied especially in connexion with the geophysical problem of seiches in lakes and other basins (Forel 1876; Kirchhoff & Hansemann 1880; White & Watson 1905–6). The most careful early experimental checks for simple shapes (circular and rectangular cylinders) appear to be those of Guthrie (1875), Rayleigh (1876), Lechat (1880), and Honda & Matsushita (1913). Much of the recent work has been concerned with extending analysis to the properties of finite-amplitude waves and the present results fall in this group.

The major point of the present paper will be introduced in a moment but it is illuminating first to describe in some detail the precise sequence of events and ideas which led to it. This sequence is an excellent example of the complex of interactions between so-called basic and so-called applied science; between theoretical, experimental, and observational results; between teaching and research; and between tactical and strategic advances that occurs in any research activity. The delicate nexus of interests and stimuli that operates in the conduct of any scientific investigation is familiar to any working scientist but it is not often any more that a case is put on the record. In the present instance, the topic is small enough that all the crucial turning points can be set down in a short space though they occurred intermittently over several years.

During the Second World War a group in the Royal Naval Scientific Service carried out studies designed to assist in the engineering design of the critical Mulberry harbours for the Normandy invasion. One of these was a calculation by a Fourier series expansion method carried to fifth-order terms of finite-amplitude two-dimensional standing waves in deep water. This calculation was published by Penney & Price in 1952 and included a heuristic estimate of the form of the probable maximum-amplitude standing wave. This estimate was to the striking

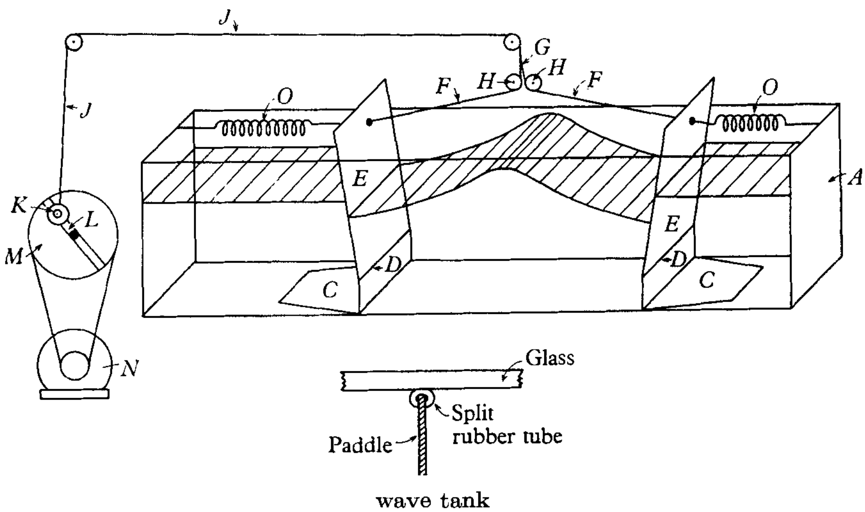

FIGURE 1. Diagram from Taylor (1953) of his arrangement for exciting standing waves in a tank. Two flap wave generators which are mechanically oscillated in opposition form the ends of the working section.

effect that the maximum wave was a sharp-crested form with a 90° angle in contrast to the Stokes (1880) result of a 120° angle for the maximum progressive wave (though in ironic coincidence with Rankine's (1865) erroneous deduction, which Stokes was concerned to correct, of a 90° angle for such waves). The finite-amplitude effect on the frequency was found by Penny & Price to be a *decrease* and, though they did not comment strongly on it, this is in interesting contrast to the frequency *increase* found by Stokes and later workers for finite-amplitude progressive waves. The 90°-crest result was met with considerable controversy and doubt which led Sir G. Taylor (1953) to undertake an experimental check. He arranged a pair of flap wave makers as shown in figure 1 from his paper so as to generate the first symmetrical standing mode (two half-wavelengths) between the flaps. He found that extremely small synchronous motions of the generator flaps were able to generate high amplitude waves when sufficiently close to resonance. At small amplitudes of water motion with a depth of 15·5 cm and tank length of 32·9 cm (i.e. a ratio of 0·471), he was able to check the theoretical inviscid period of 0·460 sec within one part in 500. For high amplitudes, he conclusively confirmed the frequency decrease predicted by Penney & Price and, with fair precision, the 90° angle. Beyond the 90°-angle maximum form he found spontaneous instabilities and transverse wave motions of the free surface setting in.

The present author became aware in 1954 of these results through Taylor's paper and commented on it to students in a theoretical hydrodynamics course in 1955 and 1956. Much later, primarily because of the precision of Taylor's period result at small amplitudes against perfect fluid theory, the author and Prof. G. W. Platzman decided to organize a teaching experiment for use in the above course and in a course in theoretical meteorology where gravitational fluid oscillations were a major theme. We procured in 1959 a rectangular aquarium for this purpose, fitted it with a single generator flap instead of two, and devised a procedure for class use. After calculation of a selection of theoretical periods, the classes determined periods up to the eighth or ninth two-dimensional modes at two or three depths. As a teaching device it turned out to be outstandingly effective, the periods agreeing always within a few tenths of a percent and a number of qualitative effects being convincingly demonstrated. For example, a little floating tracer material enabled the students to form a vivid impression of the instantaneous streamlines and of the changes in the rate of decay of the motion with depth as the depth-wavelength ratio changes for various modes. These experiments were run in April 1959 and March 1961 with some improvements the second time.

Meanwhile on the theoretical side, Prof. J. B. Keller and a visiting member, Dr I. Tadjbakhsh, of the Institute for Mathematical Sciences at New York University, partly stimulated by Penney & Price's and Taylor's work and by a general interest in free non-linear vibrations in systems with infinitely many degrees of freedom, carried out calculations by a different method of the standing waves in water of finite depth. They determined velocity potentials, surface heights, and frequencies up to second-order terms in expansions with respect to an amplitude parameter (Tadjbakhsh & Keller 1960) valid for any value of depth to wavelength ratio. The result they uncovered, which struck us, was the prediction that Penney & Price's frequency decrease (soft spring effect) would reverse to a frequency increase (hard spring effect) below a depth to wavelength ratio of 0·17. This is in marked contrast to all finite-amplitude results for progressive waves which, to the author's knowledge, call for the same sense of frequency change (increase) in shallow as in deep water. On the occasion of the last class experiment (March 1961) we decided in April to use the apparatus to check Tadjbakhsh & Keller's result. This we were able to do conclusively by May, and the details of this confirmation are the main result of this paper. During preparation of the manuscript we have been apprised by Prof. Keller of Moiseyev's (1958) theoretical discussion in which the frequency increase in shallow water has also been obtained. I am not aware of any experimental results other than Taylor's (1953) and Lin & Howard's (1960), which are for the deep water finite-amplitude case, and it therefore appeared worth while to collect our results in some detail.

Theoretical summary

The theory of infinitesimal standing waves on a perfect liquid of finite depth in a rectangular container is given by Lamb (1932). We restrict ourselves to two-dimensional motions with crest lines of the waves transverse to the long axis of the tank, and will use a dimensionless notation nearly identical with Tadjbakhsh & Keller's to facilitate comparisons. Only those formulae will be repeated that are needed for the experimental results on frequencies and for a couple of comparisons with Tadjbakhsh & Keller's theoretical expressions for the free-surface displacements. Their paper should be consulted for full details.

Dimensional quantities will be identified by a subscript $*$ and dimensionless ratios either by simple symbols following Tadjbakhsh & Keller or by a prime (′) where new symbols are needed. Let

x_* denote the horizontal co-ordinate parallel to the long axis of the tank;
y_*, the vertical co-ordinate, positive upward;
t_*, the time;
g_*, the acceleration of gravity;
λ_*, the wavelength (along x_*);
$k_* \equiv 2\pi/\lambda_*$, the wave-number;
h_*, the mean depth of the fluid;
L_*, the length of the tank;
τ_*, the period of a given mode;
and $\omega_* \equiv 2\pi/\tau_*$, the frequency of the mode.

The corresponding dimensionless quantities are

$$x \equiv k_* x_* \quad \text{and} \quad y \equiv k_* y_*,$$
$$t \equiv t_* \omega_*,$$
$$h \equiv k_* h_*,$$
and
$$\omega \equiv \omega_*(k_* g_*)^{-\frac{1}{2}};$$

ω is thus a measure of frequency in units of the short-wave frequency on deep water. In addition, $\eta_*(x_*, t_*)$ will denote the free surface displacement from the mean level $y = 0$ and a_* a measure of wave amplitude which is the amplitude of that Fourier component of the wave motion identical in type with the infinitesimal mode. The series expansion parameter with respect to which Tadjbakhsh & Keller conduct their solution is

$$\epsilon \equiv k_* a_*.$$

Further, $\epsilon\eta \equiv k_* \eta_*$ so that $\eta = \eta_*/a_*$. In the experimental data given later, it was convenient to measure the difference between the maximum and the minimum η_* at an antinode of the standing waves and to express this in units of λ_* instead of $(k_*)^{-1}$. We use $(\Delta\eta_m)_*$ for the dimensional quantity and

$$\Delta\eta_m' \equiv \frac{(\Delta\eta_m)_*}{\lambda_*} = \frac{k_*(\Delta\eta_m)_*}{2\pi}$$

for the dimensionless measure. It was not feasible, except in the special cases where the free-surface profile was measured, actually to determine a_* and ϵ.

Instead we used $\Delta\eta'_m$ which, however, is quite close to $2a_*/\lambda_* = \epsilon/\pi$ as will be seen in the cases checked.

In a tank of liquid with a given length L_*, mean depth h_*, and given breadth in the z-direction, there is a double infinity of free normal modes of oscillation. These correspond to all integer choices for the number of half-wavelengths in both the x- and z-directions that enable the boundary conditions at the walls to be satisfied. Where necessary to refer to a general mode we will use the notation (j, i) where j is the integer number of half-wavelengths in the z-direction and i is the similar number in the main x-direction. The two-dimensional modes that were actually used were mainly $(0, 2)$ with some determinations for $(0, 4)$ and $(0, 1)$. The depth of the fluid will be mainly measured by

$$h' \equiv h_*/L_*.$$

This is identical with $h_*/\lambda_* = h/2\pi$ for the most usual $(0, 2)$ mode and to $2h_*/\lambda_*$ and $\frac{1}{2}h_*/\lambda_*$ for the $(0, 1)$ and $(0, 4)$ measurements respectively.

The classical infinitesimal solution, which is the zero-order solution in Tadjbakhsh & Keller's analysis, gives for the free surface displacement

$$\eta^0 = \sin t \cos x$$

and for the frequency $$\omega_0^2 = \tanh\,(h) = \tanh\,(k_* h_*),$$

where the index 0 identifies the order of terms in their expansion. For our usual $(0, 2)$ mode the tank ends are at $x = -\pi$ and $+\pi$. For the experimental measurements of period (frequency) at various amplitudes, it was convenient to express the frequency of the (forced) standing waves as ratios to the frequency of the corresponding free infinitesimal mode. For this we use the notation

$$f' \equiv \omega/\omega_0 = \omega_*/\omega_{0*} = \tau_{0*}/\tau_*.$$

Tadjbakhsh & Keller obtain expansions of the following form in powers of ϵ for ω and η:

$$\omega = \omega_0 + \tfrac{1}{2}\epsilon^2\omega_2 + O(\epsilon^3)$$

and $$\eta = \eta^0(x,t) + \epsilon\eta^1(x,t) + \tfrac{1}{2}\epsilon^2\eta^2(x,t) + O(\epsilon^4),$$

where ω_2, η^1, and η^2 are the correction functions to the infinitesimal solution. They find

$$\omega_2 = \tfrac{1}{32}(9\omega_0^{-7} - 12\omega_0^{-3} - 3\omega_0 - 2\omega_0^5).$$

The η^1 and η^2 functions will not be quoted though they are used in the profile calculations given later. η^1 consists of two terms in $\cos 2x$ and $\cos 2t \cos 2x$ with coefficients which are determined functions of ω_0 while η^2 consists of four terms in the pairwise products of $\sin t$ and $\sin 3t$ with $\cos x$ and $\cos 3x$ and with similar coefficient functions of ω_0.

The primary result we are investigating is seen from the expression for ω_2 to give a negative ω_2 (frequency decrease from ω_0) for large ω_0 or large depth-wavelength ratios and a positive ω_2 (frequency increase) for small ω_0 or small depths. The reversal $\omega_2 = 0$ occurs at $\omega_0 \approx 0{\cdot}89$ which corresponds to $h \approx 1{\cdot}07$. This gives a depth to wavelength ratio (i.e. h' for the $(0, 2)$ mode) of $0{\cdot}17_1$. The theoretical curve of ω_2 against $h = 2\pi h'$ is given in figure 10.

Experimental arrangements and procedure

The rectangular tank used in the experiments is shown in figure 2, plate 1. It was a commercial aquarium of length $119{\cdot}1_3$ cm, breadth 38·5 cm, and height about 40·5 cm. The variations in the first two dimensions between the opposite glass walls were only $\pm 0{\cdot}02$ cm and $\pm 0{\cdot}05$ cm respectively. The base is 2·5 cm thick so that water heights are less than 38 cm. A 2·6 mm brass plate was rigidly pivoted at the bottom of the tank in such a position that its front surface was 6·1 cm from the nearest end and the value of L_* was 113·0 cm. In a manner similar to Taylor's (1953) procedure, the side edges of the plate were taped so that comparatively little fluid was able to escape past them.

A bar linkage connected the upper end of the plate to an adjustable-amplitude crank driven by an electric motor. The proportions of the linkage were such that the deviations of the plate motion from a pure sinusoid were very small for the smaller amplitudes used. The actual angular range of motion of the plate was varied over quite a large interval to generate various amplitude standing waves. The required range of motion varied from 0·0016 to 0·200 radians, being much greater for a given wave amplitude at the lower depths. For all depths except the lowest, no more than 0·09 radian was needed to reach maximum waves. At the larger depths, the plate ranges required were somewhat larger than Taylor's because only one generator flap was used instead of two.

The adjustable crank was mounted on the output shaft of a $\frac{1}{8}$-h.p. Graham variable-speed drive unit. The period variability of this drive was generally less than 10^{-3} sec with wave periods of a second or less. With careful observation the average period corresponding to a given wave condition could be determined to about one or two parts per mil. The period was measured every second or third revolution by a Beckman–Berkeley Model 7361 CKR electronic timer triggered by a capacitive detector which sensed a metal projection on the output shaft. The accuracy of this measurement (10^{-5} sec) is so much greater than the motor stability that no sensible error occurs due to it. The two prime reasons for the easy feasibility of the observations were the convenience and accuracy of the time measurement and the stability and continuous variability of the Graham drive.

The liquid used in the tank was tap water at near room temperatures of 16–22 °C. A concentration of 10^{-3} by volume of Kodak Photoflo detergent was added to improve the surface behaviour and reduce capillary effects. The surface tension value was thence about 30 dynes/cm as against the pure water value of about 71 dynes/cm. The depths of water used in the tank were 22·60, 16·95, 14·69, and 11·30 cm corresponding to h' values of 0·20, 0·15, 0·13 and 0·10. For the (0, 2) mode the values of h_*/λ_* are the same. Determinations were carried out for for the (0, 4) mode at $h' = 0{\cdot}20$ and for the (0, 1) mode at $h' = 0{\cdot}10$ giving h_*/λ_* values of 0·40 and 0·05 respectively. The absolute values of the mean depths are probably not more precise than $\pm 0{\cdot}02$–$0{\cdot}03$ cm but care was taken to see that the depth was constant in each series to $\pm 0{\cdot}01$ cm. The theoretical infinitesimal wave periods and frequencies corresponding to these depths and the adopted dimensions are given in table 1.

As will be seen from later figures, the values of frequency or period extrapolated to small amplitudes usually differed from the theoretical values by only 0·2–0·3 % though one or two are as large as 0·5 %. These differences are most likely due to absolute depth errors or to slight changes in the effective length of the tank at the moving flap. Both direct viscous and surface tension effects on the infinitesimal-wave periods are very small for the dimensions involved here.

h'	Mode	h	$\tau_*(s)$	$(K_* g_*)^{\frac{1}{2}}(s^{-1})$	ω_0	ω_2 obs.	ω_2 theor.
0·20	(0, 4)	2·51	$0{\cdot}605_8$	$10{\cdot}44_1$	$0{\cdot}993_5$	$-0{\cdot}3_1$	$-0{\cdot}242$
	(0, 2)	$1{\cdot}25_6$	$0{\cdot}923_3$	7·383	$0{\cdot}922_0$	$-0{\cdot}2_6$, $-0{\cdot}2_8$	$-0{\cdot}11_0$
0·170	(0, 2)	1·07	$0{\cdot}958_0$	7·383	$0{\cdot}888_1$	$-0{\cdot}11$, $-0{\cdot}09$	$-0{\cdot}00_8$
0·15	(0, 2)	$0{\cdot}94_2$	$0{\cdot}992_0$	7·383	$0{\cdot}858_1$	$-0{\cdot}05_0$	$0{\cdot}11_8$
0·13	(0, 2)	$0{\cdot}81_7$	$1{\cdot}037_4$	7·383	$0{\cdot}820_6$	$0{\cdot}07_5$	$0{\cdot}34_4$
0·115	(0, 2)	$0{\cdot}70_1$	$1{\cdot}082_1$	7·383	$0{\cdot}786_5$	0·30, 0·45	$0{\cdot}64_7$
0·10	(0, 2)	$0{\cdot}62_8$	$1{\cdot}140_7$	7·383	$0{\cdot}746_3$	0·5, 0·8	$1{\cdot}1_9$
	(0, 1)	$0{\cdot}31_4$	$2{\cdot}181_5$	5·220	$0{\cdot}551_6$	6·5	15·7

TABLE 1

The procedure, like Taylor's (1953), and Lin & Howard's (1960), consisted of setting the wave generator to a given range and measuring the equilibrium wave heights (crest to trough difference) at a series of closely spaced frequencies (periods) ranging from 5 % above to 5 % below the infinitesimal-wave value. This procedure was repeated for half a dozen or so wave generator ranges, the highest being usually sufficient to reach the unstable maximum-wave forms. The oscillator periods, as already mentioned, were measured with more than sufficient accuracy but the drive variations introduced the principal problem of determining a valid average period at an equilibrium condition of the waves simultaneous with the height measurement. The height measurement was always taken at the central antinode of the standing wave except for the (0, 1) mode where it was taken at the tank end opposite the generator flap. It was made by visual estimate against a millimeter rule placed on the glass front with one index at the mean level of the water. When the tank and background were lighted properly the bottom of the meniscus appeared as a sharp line whose position could be read to within $\frac{1}{4}$–1 mm depending on the height of the waves (less accurately for high amplitudes).

Experimental results

The results of these measurements are given in figures 3–9 as curves of $\Delta\eta'_m$ the wave height in units of λ_* against f', the observed frequency in per cent of the small-amplitude theoretical frequency. These curves of amplitude-frequency for the forced response of the fluid are similar to those of Taylor (1953) and Lin & Howard (1960), except that Taylor used the crest height above mean level in units of λ_* and Lin & Howard used a dimensionless crest-trough distance for which 1·0 corresponds to $\Delta\eta'_m = (2\pi)^{-1} = 0{\cdot}15_9$.

Using figure 3 as an example, the response curves show the same overlap between low- and high-frequency branches of the curve that Taylor found except

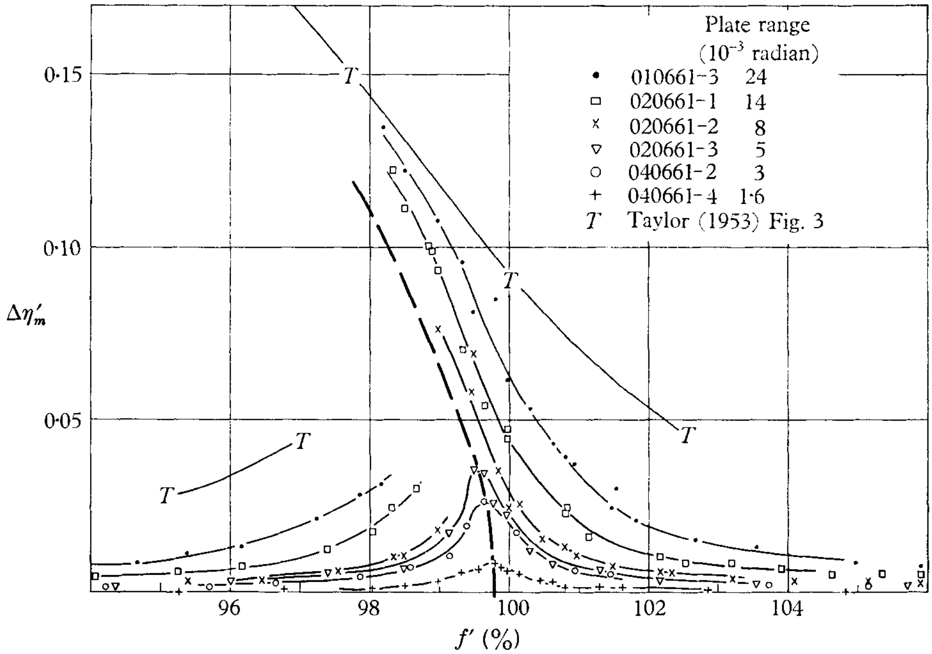

FIGURE 3. Curves of the total wave amplitude $\Delta\eta'_m$ (in units of λ) against frequency f' (in per cent) of the infinitesimal-wave frequency for various ranges of motion of the generator flap (given in units of 10^{-3} radians). Measurements for the (0, 4) mode at $h' = 0{\cdot}20$ ($h_*/\lambda_* = 0{\cdot}40$). Curves marked T are transcribed from Taylor (1953) using approximate factors from figure 11. The dashed curve is the estimated free-mode frequency-amplitude curve and gives an estimated ω_2 of $-0{\cdot}3_1$ *vs* a theoretical $\omega_2 = -0{\cdot}24$.

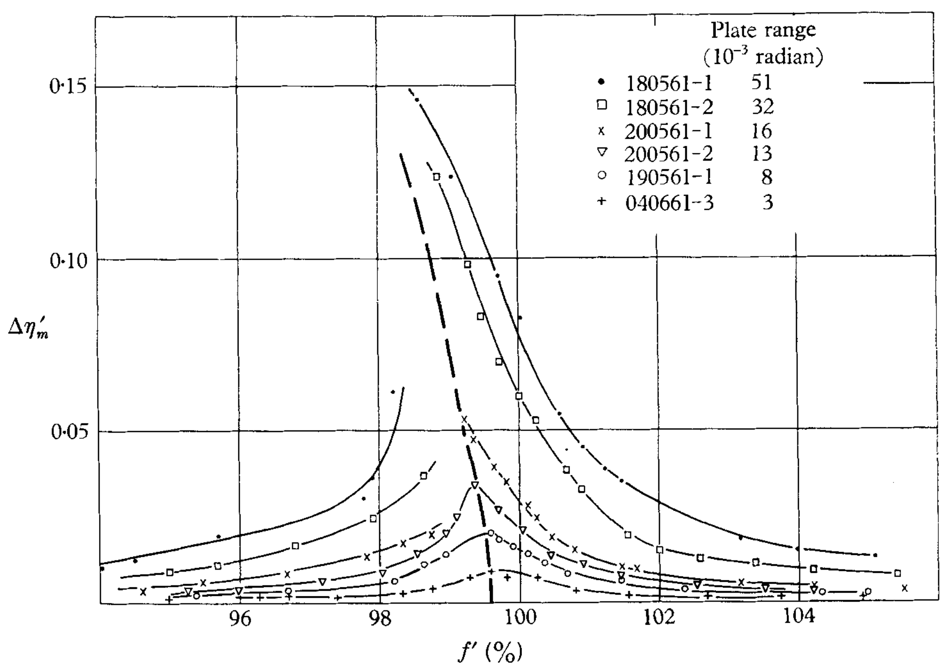

FIGURE 4. Curves similar to figure 3 for the (0, 2) mode at $h' = 0{\cdot}20\,(h_*/\lambda_* = 0{\cdot}20)$. Estimated ω_2 values -2_6, $-0{\cdot}2_8$ *vs* theoretical $\omega_2 = -0{\cdot}11$.

at low amplitudes. Parts of Taylor's curves for $h_*/\lambda_* = 0{\cdot}47_1$ (figure 3, Taylor 1953) have been placed on figure 3 using an approximate conversion from the crest height to total wave height ratios given in figure 11. Lin & Howard, in part of their investigation, actually computed the forced response of an inviscid liquid by an expansion procedure similar to Tadjbakhsh & Keller's taking approximate account of the motion of their flap wave generator. They obtained excellent agreement of the computed frequency-amplitude curves with their observations. We will not enter into the very difficult questions of the interpretation of these curves taking account of the actual forcing and the viscous and capillary effects that actually determine them. A complete discussion is beyond any theory that has yet been carried through, and Lin & Howard's results suggest that the latter effects are not important for waves generated in the present manner. Instead we will assume that a curve drawn in the general manner of the dashed curve in figure 3 will approximate the frequency-amplitude behaviour of a strictly free standing oscillation in perfect fluid. Such an assumption agrees qualitatively with the relation of Lin & Howard's results for free as against forced response and with Penney & Price's free calculation as against Taylor's observed curves.

With the above assumption we can now follow the changes in the estimated free-oscillation frequency curve through the series of depths on which we have made measurements. On figure 3 at $h_*/\lambda_* = 0{\cdot}40$ there is quite close agreement with Taylor's (1953) and Lin & Howard's (1960) results at greater depth ratios. In figure 4 at $h' = h_*/\lambda_* = 0{\cdot}20$ the appearance is similar, but close comparison shows that the frequency change with amplitude is perceptibly smaller in magnitude. In figures 5 and 6 at $h' = h_*/\lambda_* = 0{\cdot}17$ and $0{\cdot}15$ the frequency changes are much less but are still distinctly in the direction of a decrease up to $\Delta\eta'_m$ about $0{\cdot}07$ or $0{\cdot}10$. $h' = 0{\cdot}17$ was checked, of course, because of its near coincidence with Tadjbakhsh & Keller's predicted reversal value. However, the highest amplitudes attained in figure 6 show a very interesting and distinct shift to higher frequencies. When we proceed to figure 7 at $h' = h_*/\lambda_* = 0{\cdot}13$ the frequency change is definitely an increase though there is still a faint suggestion of a frequency decrease up to $\Delta\eta'_m$ about $0{\cdot}02$.

Figures 5–7 conclusively confirm Tadjbakhsh & Keller's (1960) and Moiseyev's (1958) prediction of a frequency increase in shallow water but place the reversal fairly distinctly at a lower value than the predicted $h_*/\lambda_* = 0{\cdot}17_1$. Figures 7 and 8, though not carried to as large amplitudes, exhibit the increase in magnitude of the frequency rise as h_*/λ_* is reduced to $0{\cdot}10$ and $0{\cdot}05$. In addition, curves were obtained for $h_*/\lambda_* = 0{\cdot}115$. They lie between the $0{\cdot}13$ and $0{\cdot}10$ values and the corresponding ω_2 estimates appear in figure 10. It will be noted from the angular range values for the flap that are given on the figures, that much larger ranges were required for a given $\Delta\eta'_m$ at the shallower depths. This is due to a number of causes but probably most importantly to the fact that, in shallow water, a piston-type generator instead of a flap is the proper type for coupling to the free modes.

One further point should be mentioned. Very late in the series of measurements it was noticed that some slight play was present in the drive linkages sufficient to produce a fraction of a millimetre looseness in the plate drive. It was decided to complete the series without changing any of the conditions. At the end, however,

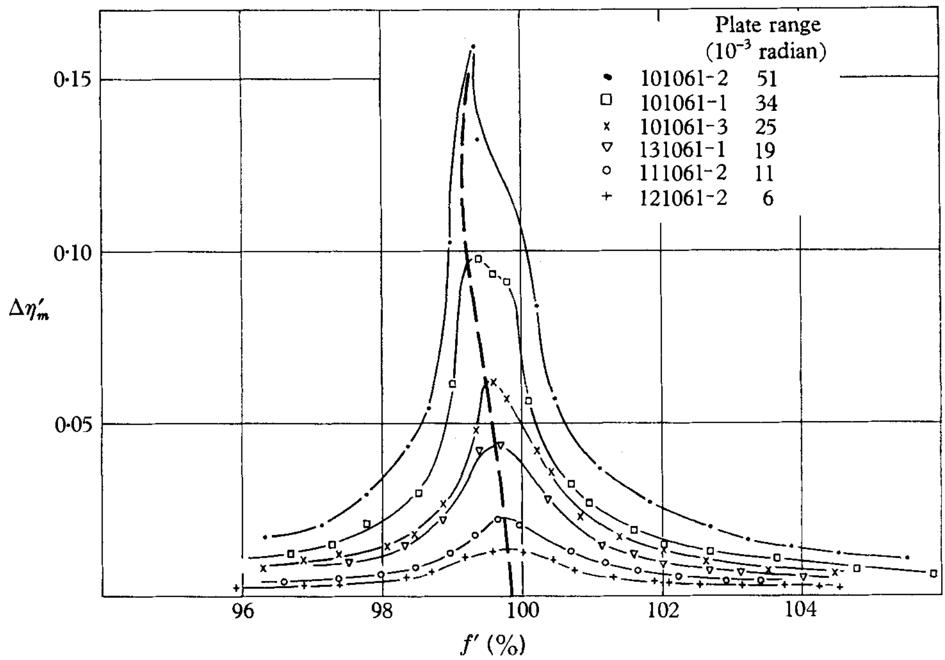

FIGURE 5. Curves similar to figure 3 for the (0, 2) mode at $h' = 0{\cdot}17$ near Tadjbakhsh & Keller's theoretical frequency reversal point. Estimated $\omega_2 = -0{\cdot}11, -0{\cdot}09$ *vs* theoretical $\omega_2 = 0$. The change of trend of the free frequency-amplitude curve from figure 3 is very distinct by now.

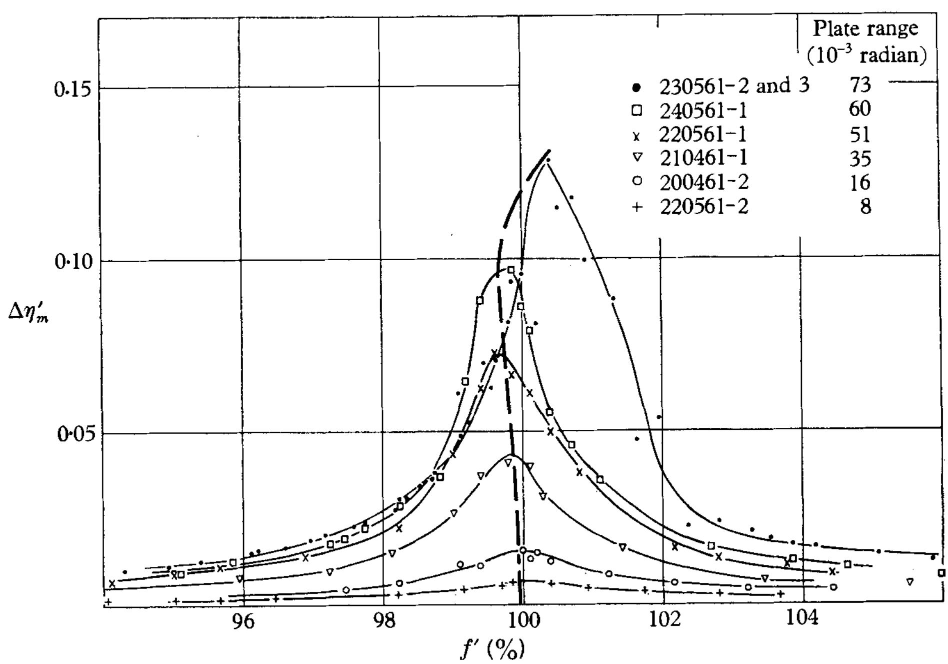

FIGURE 6. Curves similar to figure 3 for the (0, 2) mode at $h' = 0{\cdot}15$. Note the distinct shift to higher frequency above $\Delta\eta'_m \sim 0{\cdot}10$. Estimated ω_2 from the lower portion of the dashed curve $-0{\cdot}05$ *vs* theoretical $\omega_2 = +0{\cdot}12$.

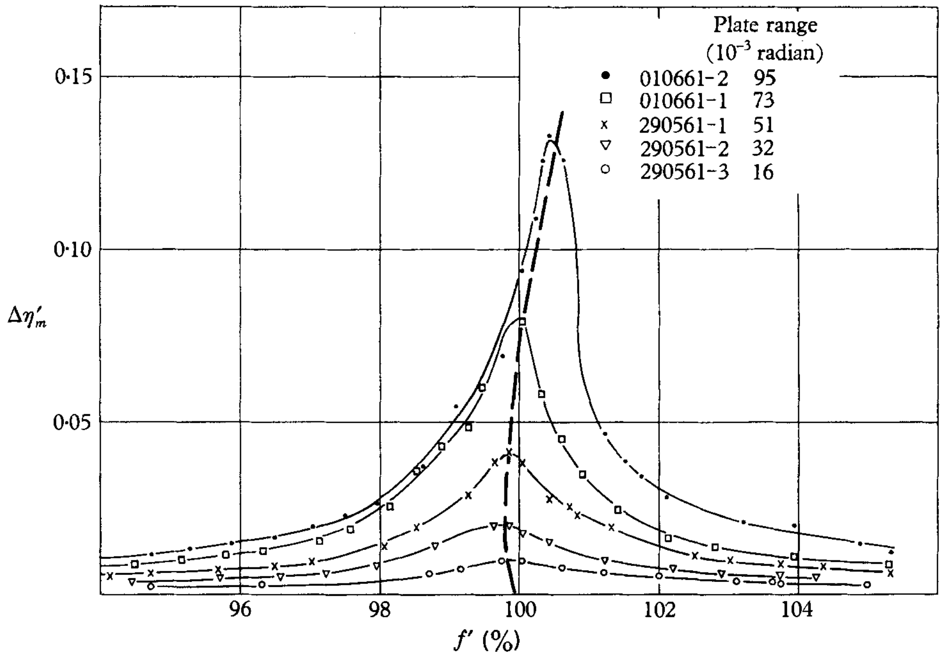

FIGURE 7. Curves similar to figure 3 for the (0, 2) mode at $h' = 0{\cdot}13$. By now at the higher amplitudes the dashed curve definitely trends toward higher frequency but the two lowest response curves in the original data, though the maxima are flat, show a fairly definite shift toward lower frequency. Estimated ω_2 from the upper portion of the dashed curve $+0{\cdot}07_5$ *vs* theoretical $\omega_2 = +0{\cdot}36$.

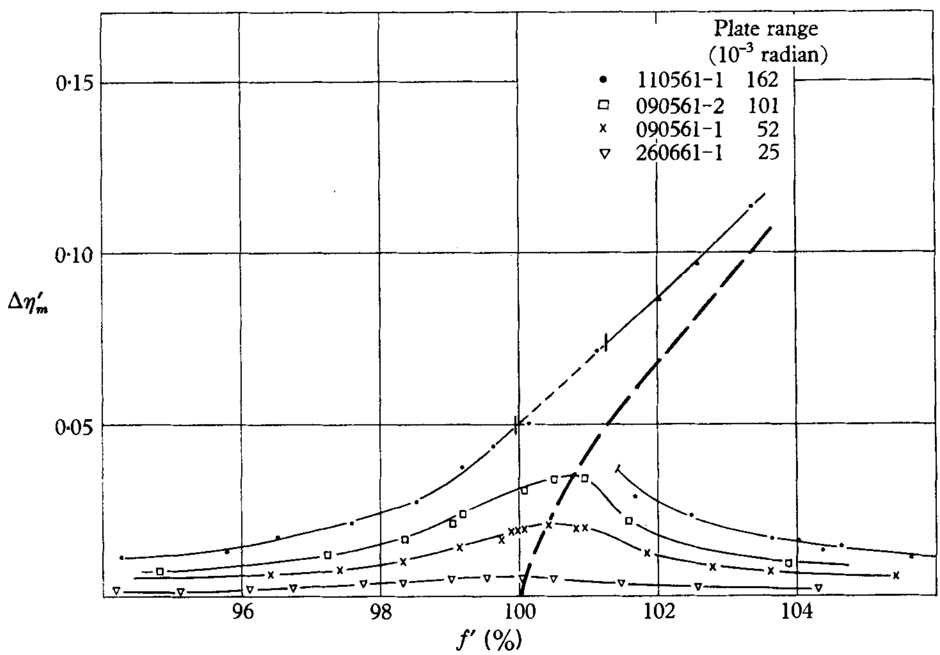

FIGURE 8. Curves similar to figure 3 for the (0, 2) mode at $h' = 0{\cdot}10$. The shift to high frequency is now unmistakable even though the lowest response curve is very flat. The dashed portion of the topmost response curve is a zone where the standing wave was quite unstable and not regularly periodic. Estimated ω_2 values $+0{\cdot}5$, $0{\cdot}8$ *vs* theoretical $\omega_2 = 1{\cdot}20$.

the pivot points were reworked to produce no noticeable play. One critical curve was rechecked with the result that the peak point was unaltered but the curve was slightly narrower, amplitudes being slightly lower on either side of the maximum. We do not believe, within the general accuracy described later, that any serious alterations in results would arise from this correction. Probably some of the disturbance harmonics in later profiles would have been less prominent.

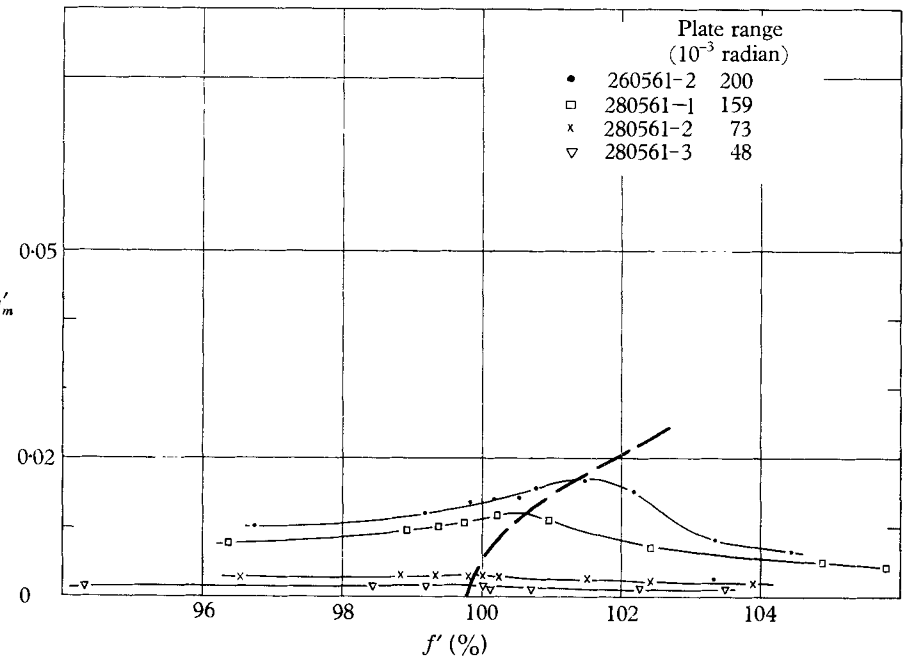

FIGURE 9. Curves similar to figure 3 for the (0, 1) mode at $h' = 0{\cdot}10(h_*/\lambda_* = 0{\cdot}05)$. Here the generator flap motions required were so large that the unstable maximum wave could not be reached. Note that the $\Delta\eta'_m$ scale has changed, the waves are very flat, and the frequency effect very large. Estimated ω_2 value 6·5 *vs* theoretical $\omega_2 = 15{\cdot}7$.

We have made an attempt to estimate experimental values of the coefficient ω_2 in the expansion for frequency from figures 3 to 9 and a few data that have not been given. Such an estimate is made uncertain by the fact that the relation between $(\Delta\eta_m)_*$ and Tadjbakhsh & Keller's amplitude parameters a_* and ϵ has been determined only in the few cases where we have measured the surface profile and determined its Fourier representation. In these cases, considered in the next section, a_* is the dimensional amplitude of the lowest harmonic in x.

We will consider the complications below, but as an approximation decided to calculate ω_2 treating $(\Delta\eta_m)_*$ as equal to $2a_*$, the linear solution value. This implies $\Delta\eta'_m = \epsilon/\pi$. In any case, to the order of Tadjbakhsh & Keller's calculation, the free-mode curve is a parabola on the frequency-amplitude diagrams of figures 3–9. The type of behaviour on figure 6 suggests that a parabola should not be fitted up to too-large values of $\Delta\eta'_m$ but, since the accuracy with which the free frequency curves are defined is not too high, we were forced to take a fairly large interval. There was also the problem of the few tenths per cent differences between the limiting small-amplitude trend of the dashed curves in figures 3–9 and the 100 % f' value.† The values of ω_2 in figure 10 were finally obtained by calculation from the frequency difference using two points on the dashed curves: those at $\Delta\eta'_m = 0$ and at either 0·10, 0·05, or 0·015 in the case of figure 9. In some cases, values from both 0·10 and 0·05 are given in table 1 and figure 10. Tadjbakhsh & Keller's limiting value for deep water is $\omega_2 = 0{\cdot}25$ and this is

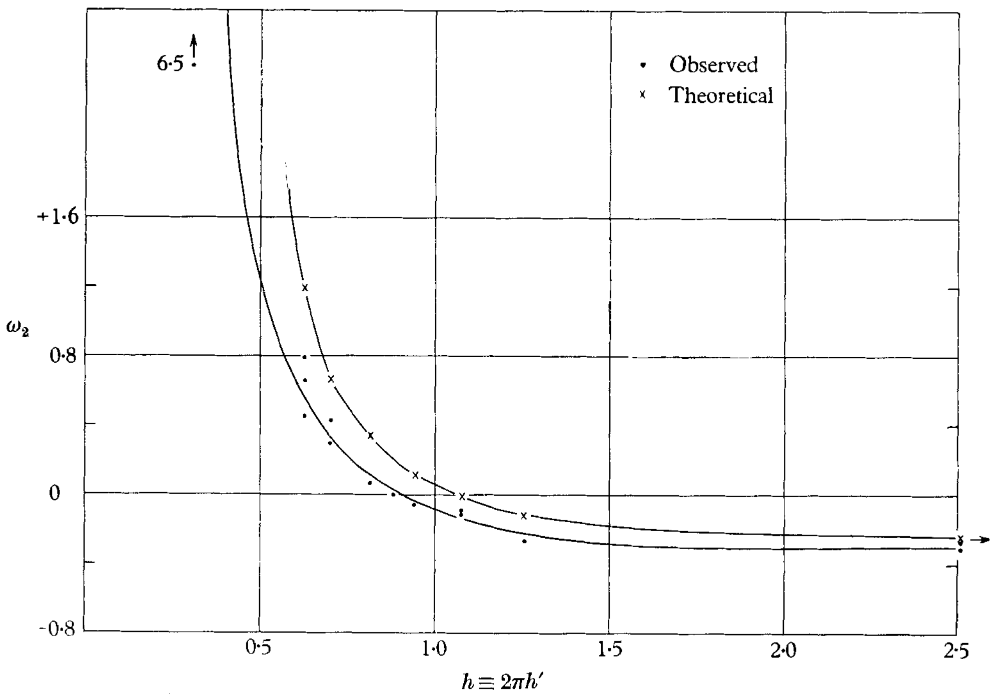

FIGURE 10. Theoretical and estimated observed curves of ω_2 versus depth $h \equiv 2\pi h'$.

in quite close agreement with both Taylor's observations and some of Lin & Howard's results. In general, figure 9 shows that the estimated values lie systematically below the theoretical ω_2's; hardly by a significant amount in the deepest case but increasingly toward the shallow end. In particular, the $\omega_2 = 0$ value is rather sharply fixed by the observed cases at a value very near $h' = 0{\cdot}14$ ($h = 0{\cdot}88$) where the theoretical value is $\omega_2 = +0{\cdot}2$. One cannot give so much weight to the ω_2 values for the two lowest depths but the differences still seem large enough to be real. It is hardly possible to give a realistic estimate of the precision of these ω_2 measurements but, aside from the problem of the difference between $(\Delta\eta_m)_*$ and $2a_*$, ± 30–50 % is probably conservative.

Purely to facilitate comparisons with data such as Taylor's (1953) in which the crest height above mean level is used, figure 11 gives a collection of observations of the ratio of crest height η'_+ (units of λ_*) to the wave height $\Delta\eta'_m$ plotted against

† In passing it is interesting to note, as a close inspection of the data points in figures 3–9 shows, that detectable frequency changes of 0·2–0·5 % occur on the low-amplitude curves with total wave heights of as little as 0·02–0·04 of λ_*.

$\Delta\eta'_m$ itself. These observations are very inaccurate below $\Delta\eta'_m \sim 0{\cdot}05$ (to left of the wavy line) but above that value are fairly reliable. The indicated rise in this ratio for $h_*/\lambda_* = 0{\cdot}20$ near $\Delta\eta'_m = 0{\cdot}025$ was fairly consistent but no obvious explanation is apparent. It is also interesting and probably significant that at the more reliable wave heights the ratio of crest to wave height is a minimum near $h_*/\lambda_* = 0{\cdot}15$ where the frequency effect reverses and is greater for both smaller and larger depths.

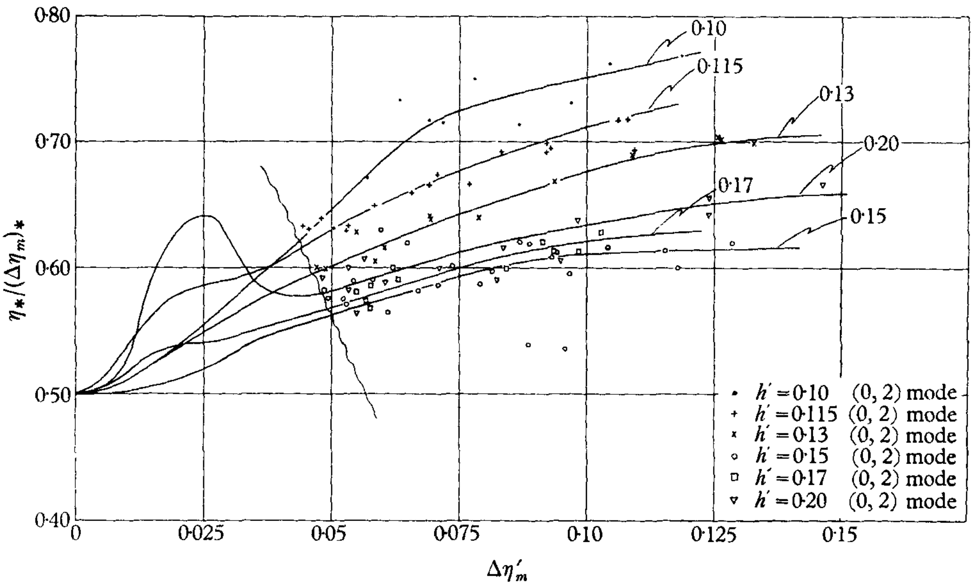

FIGURE 11. Curves of the ratio of crest height to wave height $\eta_*/(\Delta\eta_m)_*$ against $\Delta\eta'_m$ for various depths. There is a large scatter of the observed points below $\Delta\eta'_m$ about 0·05 between ratios of 0·50 and 0·60. The measurements are not sufficiently precise to say whether the indicated humped curves are real. At larger wave heights, the ratio measurements are fairly consistent and indicate an interesting minimum of the ratio near $h_*/\lambda_* = 0{\cdot}15$.

Before proceeding to the next section, in which the details of the wave profiles will be discussed briefly, it is interesting to consider some aspects of the free-mode amplitude-frequency curves as they have been sketched in figures 3–9. Taken at their face value, for moderate wave heights (say 0·05–0·10) where the measurements are conclusive, they show the frequency effect reversal near $h_*/\lambda_* = 0{\cdot}14$ that has already been described. The difference from Tadjbakhsh & Keller's prediction must either be correct or be produced by some such failures to produce correct finite-amplitude free modes as are discussed below in connexion with the wave profiles. If correct and if Tadjbakhsh & Keller's calculation is assumed correct as far as they carry it, then the following appears necessary: in the range of h_*/λ_* between say 0·18 and 0·12, Tadjbakhsh & Keller's calculation can be accurate in predicting the frequency change precisely (say to 0·05 %) only up to very low $\Delta\eta'_m$ values of 0·01–0·02 and the rest of the free-mode frequency-amplitude curves must depend on higher order terms. At such low $\Delta\eta'_m$ values, the experimental estimates certainly are not sufficiently precise to rule out such a

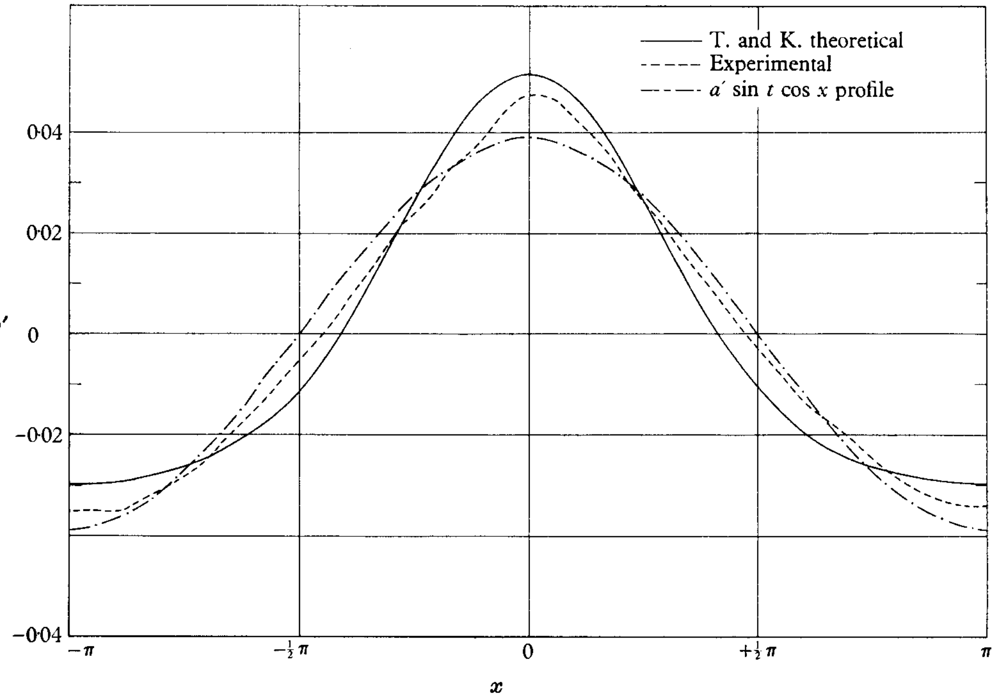

FIGURE 13. Measured surface profile height in λ_* units of the photograph in figure 12a (plate 1). Observed profile (dashed curve), theoretical profile (full curve), and cosine curve with amplitude a' (dash-dot curve). Compare Fourier coefficients in table 2.

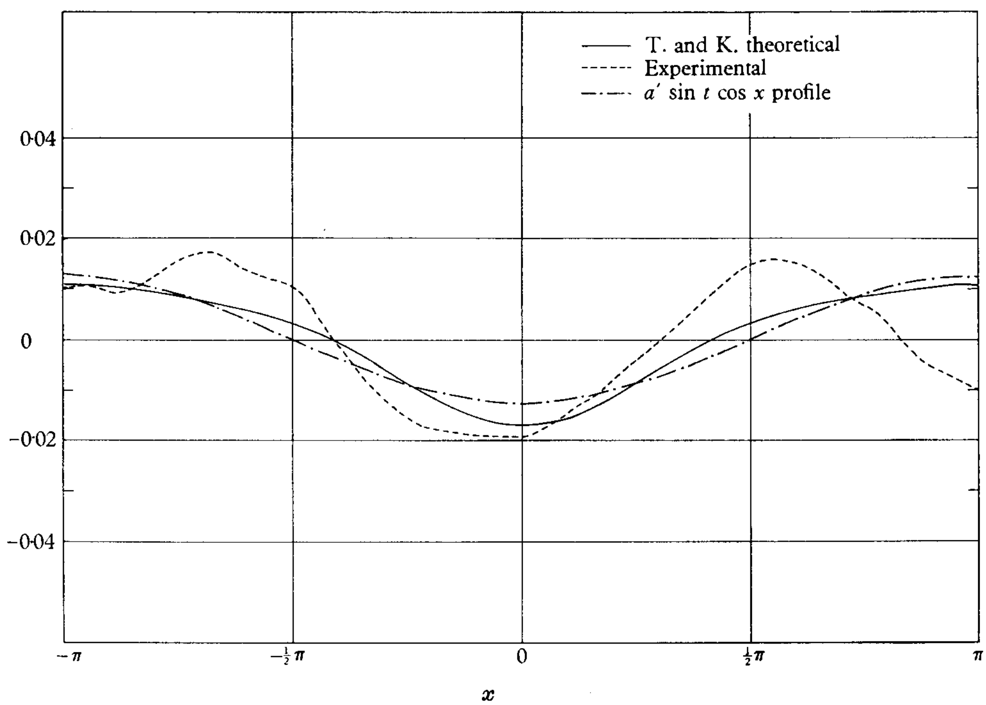

FIGURE 15. Measured surface profile height in λ_* units of the photograph in figure 14c (plate 2). Observed profile (dashed curve), theoretical profile (full curve), and cosine curve with amplitude a' (dash-dot curve). Compare Fourier coefficients in table 2.

possibility. On figures 6 and 7, at $h_*/\lambda_* = 0{\cdot}15$ and $0{\cdot}13$ respectively, for example, this would mean that the free frequency-amplitude curve first should trend to the right in accordance with the theoretical ω_2 but then trend to the left and finally to the right as amplitude increases. At least at some depths, this would produce two finite amplitudes having zero frequency change from the infinitesimal wave value. It would certainly be valuable for the calculations to be carried to one or two higher orders than Tadjbakhsh & Keller have done in order to see whether such results appear theoretically.

Wave profiles

Figure 12, plate 1, and figure 14, plate 2, give photographs of the wave profiles for (0, 2) modes which, even though for various accidental reasons we did not obtain photographs of as pure standing modes as many involved in the previous measurements, illustrate some interesting points for moderate ($h_*/\lambda_* = 0{\cdot}20$) and low ($h_*/\lambda_* = 0{\cdot}10$) depths. The photographs given are selected from a series of high-speed flash photographs taken for short intervals of time at repetition rates of about 5–6 per sec so that several photos are obtained per wave period. A reasonably precise transparent grid with blocks 10 cm on a side was fastened to the front of the tank. On five negatives, two of which are included in these figures, comparator measurements of the wave profile η_* were made at thirty-six x-stations by a differencing procedure against the grid lines as references. A Fourier analysis with respect to $\cos nx$ and $\sin nx$ of these measurements was then carried out on a Univac I computer using a programme originally prepared for meteorological-type data by R. E. Kaylor.

It was possible by careful comparison of the $\frac{1}{100}$ sec timer readings appearing in the photos with the wave shapes to assign a time origin and conversion to Tadjbakhsh & Keller's dimensionless t. We measure an equivalent time in angular degrees which at the extreme crest position at the tank centre when the water is instantaneously stationary has the value 90°. From the Fourier analysis it was then possible to derive a value of a_* or $a' \equiv a_*/\lambda_*$ corresponding to Tadjbakhsh & Keller's amplitude parameter and to compute the theoretical profile for the

---

Explanation of plate 1

Figure 2 (plate 1). Photograph of the aquarium used for the measurements. The generator flap pivoted at the bottom is seen just to the right of the front left corner of the tank. The Graham motor, adjustable crank, and linkage are in the left foreground. The Beckman electronic timer is in the rack in the background.

Figure 12a (plate 1). High-speed flash photograph (080661–2–14) of (0, 2) mode in the tank at time $t \approx 90°$ with mean depth $h_*/\lambda_* = 0{\cdot}20$. Conditions: oscillator period $= 0{\cdot}935$ sec, $f' = 0{\cdot}988$, $\Delta\eta'_m \sim 0{\cdot}07_3$, plate range $= 0{\cdot}024$ radians, photograph on Kodak Plus-X Pan 35 mm film, camera Robot Royal III, 30 mm lens at $f/11$, lens at mean water level and 69 in. from front of tank, flash tubes nominal 56 Ws total.

Figure 12b (plate 1). High-speed flash photograph (080661–2–15) of (0, 2) mode at time $t \approx 171°$, 0·21 sec after figure 12a. Note the distinct flattening of the central crest. Conditions as figure 12a.

Figure 12c (plate 1). High-speed flash photograph (080661–2–17) of (0, 2) mode at time $t \approx 321°$, 0·39 sec after figure 12b. Conditions as figure 12a.

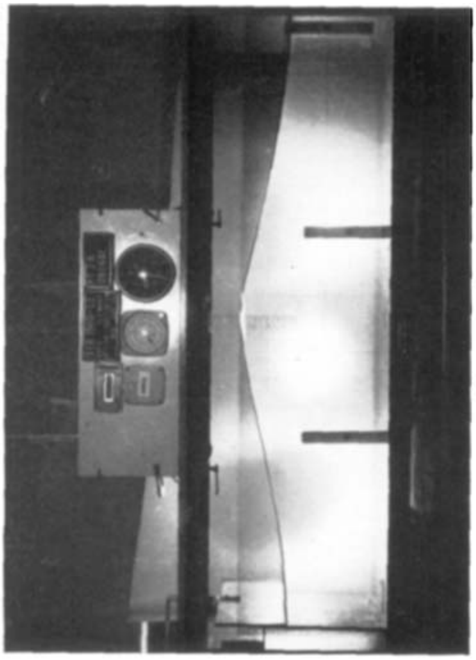

FIGURE 12*a*

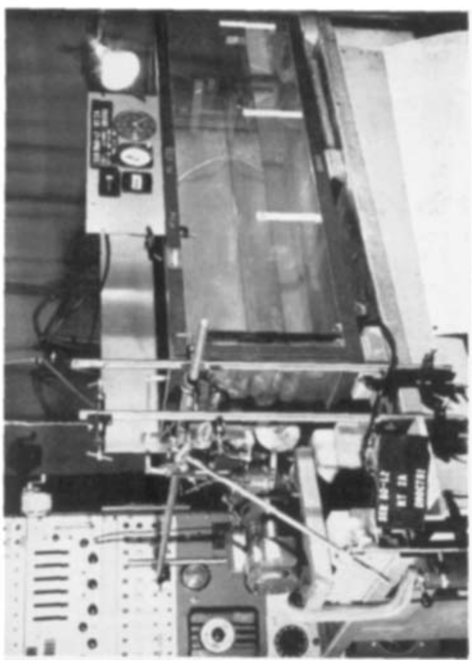

FIGURE 2

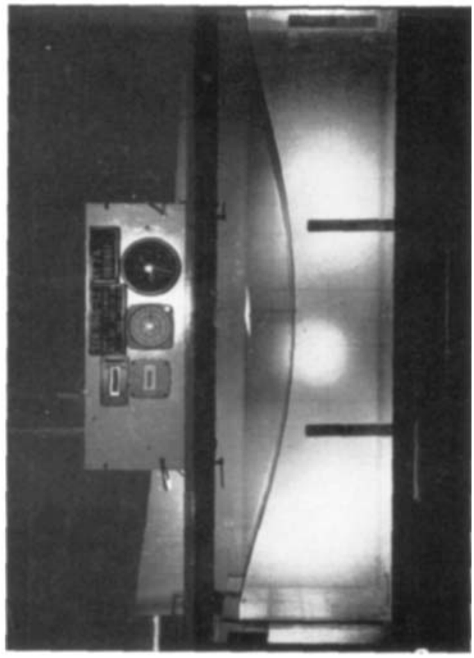

FIGURE 12*c*

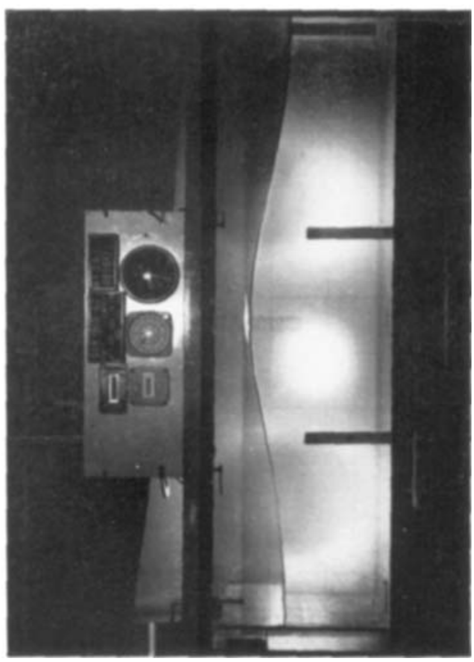

FIGURE 12*b*

(For legends see facing page)

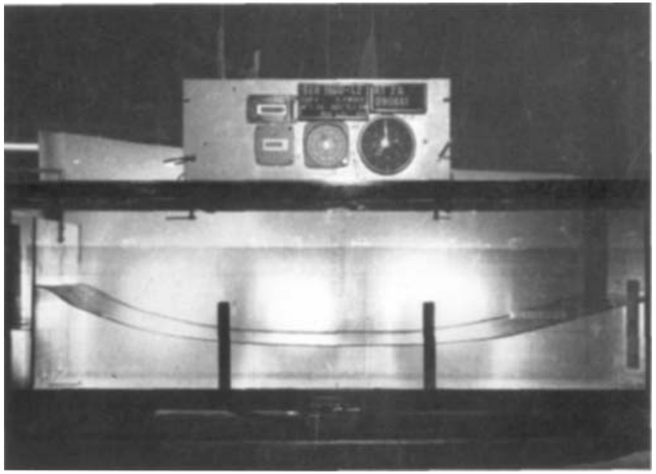

FIGURE 14a

FIGURE 14a (plate 2). High-speed flash photograph (090661–4–15) of (0, 2) mode in the tank at time $t \approx 295°$ with mean depth $h_*/\lambda_* = 0{\cdot}10$. Conditions: oscillator period = 1·11 s, $f' = 1{\cdot}027$, $\Delta\eta'_m$ uncertain 0·10–0·11$_5$, plate range 0·16 radian, camera as figure 12a (plate 1), except lens 11·3 cm above mean water level.

FIGURE 14b (plate 2). High-speed flash photograph (090661–4–17) of (0, 2) mode at time $t \approx 68°$, 0·41 sec after figure 14a. Note the distinct asymmetry in these two photos and small disturbance harmonics greater than in figures 12a, b and c. Conditions as figure 14b.

FIGURE 14c. (plate 2). High-speed flash photograph (090661–4–19) of (0, 2) mode at time $t = 198°$, 0·40 sec after figure 14c. The increased harmonic content at this shallower depth is clearly evident in the two crests at left and right which are identifiable for some time as individual crests moving from the centre toward the ends. Conditions as figure 14a.

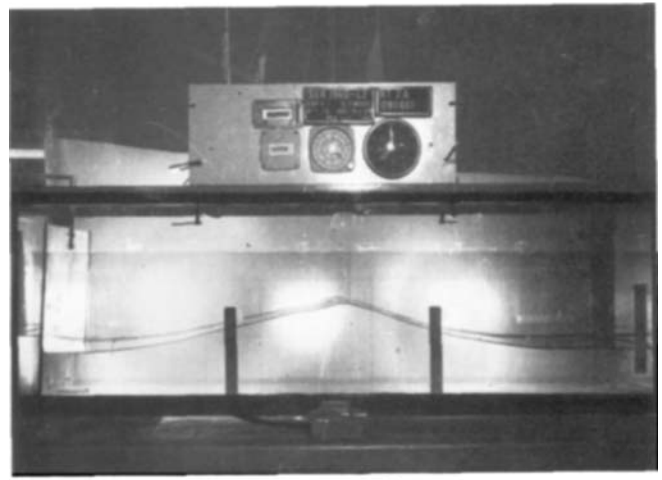

FIGURE 14b

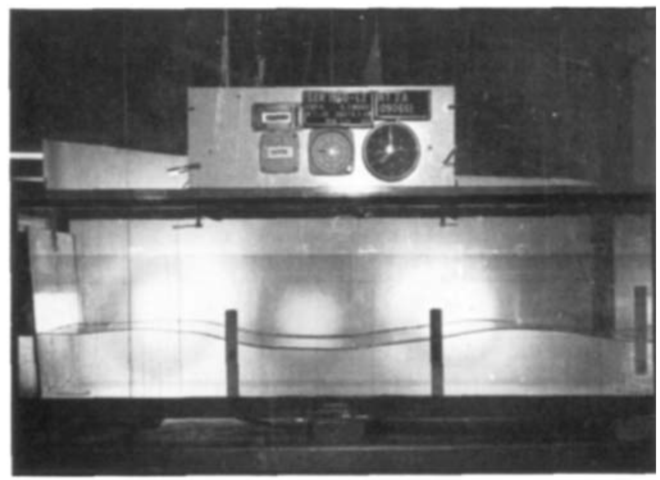

FIGURE 14c

photograph time. Values of the theoretical and observed Fourier components are given in table 2 and comparisons of the profile curves for the photos in figure 12*a*, plate 1, and figure 14*c*, plate 2, are given in figures 13 and 15. All the amplitudes are measured in units of $10^{-3}\lambda_*$ (i.e. one unit is slightly over 1 mm.). The theoretical cosine amplitudes given were obtained by fitting the zero-order term in

Photo	$\Delta\eta'_m$ (10^{-3} units)	a' (10^{-3} units)	n	Obs. cosine coeff's. (10^{-3} units)	Theor. cosine coeff's. (10^{-3} units)	Obs. sine coeff's. (10^{-3} units)
080661–2–14,	73	34·2	1	34·2	34·2 + 0·3	1·6
$h' = 0{\cdot}20$,			2	4·1	9·7	−0·1
$t = 90°$			3	1·7	1·5	0·6
			4	0·7	—	0·3
			5	0·4	—	0·2
			6	0·4	—	0·4
090661–5–35,	94	38·2	1	35·9	35·9 + 0·6	1·3
$h' = 0{\cdot}13$,			2	7·0	9·8	0·4
$t = 111° 15'$			3	2·6	2·1	−0·5
			4	2·1	—	−0·4
			5	1·0	—	−0·6
			6	0·1	—	−0·9
090661–5–30,	94	41·9	1	41·5	41·5 + 0·5	0·8
$h' = 0{\cdot}13$			2	13·0	14·1	−0·8
$t = 96° 24'$			3	5·5	2·7	−0·1
			4	2·7	—	0·1
			5	0·2	—	−0·6
			6	0·6	—	−0·1
090661–5–38,	94	40	1	−5·2	−5·2–0·3	−0·9
$h' = 0{\cdot}13$,			2	−7·7	−7·4	−1·1
$t = 352° 32'$			3	3·2	−0·4	−0·5
			4	−0·3	—	−0·1
			5	−0·4	—	0·2
			6	1·4	—	−0·1
090661–4–19,	100–115†	36·2	1	−11·1	−11·1–0·5	1·2
$h' = 0{\cdot}10$,			2	−8·8	−2·8	4·7
$t = 197° 50'$			3	1·8	−0·7	−1·7
			4	0·9	—	1·1
			5	−0·6	—	−1·1
			6	0·2	—	0·5

† Very uncertain.

TABLE 2

Tadjbakhsh & Keller's expansion, allowing for the time factor, to the observed $n = 1$ coefficient. The added fraction for $n = 1$ arises from a second-order term in $\cos x$ in the theoretical profiles.

On the question referred to earlier of the differences between $\Delta\eta'_m$ and $2a_*/\lambda_*$ which affect the experimental estimates of ω_2, the last two photographs in table 2 are not much help because the fundamental $\sin t \cos x$ has a small $\sin t$ value and the values of t are not sufficiently accurate to calculate reasonably accurately back to a_*. But the first three near $t = 90°$ or $\frac{1}{2}\pi$ (i.e. at maximum crest height) and with relatively large wave heights give some indication. $\Delta\eta'_m$ is greater than $2a_*/\lambda_*$ (by an amount that clearly must be larger the larger the wave height) and these three photos give excesses of the order of 10–20 %. The effect on the ω_2 values in figure 10 or table 1 would be to increase the magnitudes regardless of sign by amounts, if anything, less than 20–40 % (depending on the weight of the lower amplitudes in determining the free-mode frequency-amplitude curves). On figure 10 this would tend to rotate the curve for the observed estimate clockwise.

One of the features of Penney & Price's (1952) and of the later non-linear analyses of standing waves is that, while there are times ($t = \frac{1}{2}\pi, \frac{3}{2}\pi$) when the disturbance velocity field identically vanishes and the disturbed surface height is an extremum, there are no times when the height disturbance is identically zero. The $\cos 2x$ and $\cos 3x$ harmonics in η^1 and η^2 occur multiplied by sinusoidal time functions with phase differences so that all the latter do not vanish at once. These conclusions are found valid experimentally for all wave heights $\Delta\eta'_m$ above quite low values (0·03–0·05). One notices, for example, the time phase differences for larger wave heights, when the main (0, 2) crest is falling, in a flattening at the antinode (figure 12*b*, plate 1) so that two relative crests occur due to time lag of the higher harmonics in reaching their maxima. Thus in contrast to the infinitesimal waves where the wave shape is self-similar in time, the finite waves vary their shape periodically.

Also in agreement with Tadjbakhsh & Keller's results is the general observation that for low depths such as $h_*/\lambda_* = 0{\cdot}15$, 0·13 and 0·10, the higher harmonics are more prominent and even produce extra crests in the total wave profile at some phase times. Figure 14*c*, plate 2, at an $h_*/\lambda_* = 0{\cdot}10$ is an example with a strong double peak at a time t of 197° 50′. In fact in this case the observed impression, through most of a wave period, is that these extra crests are identifiable as progressive waves proceeding from centre to ends and back. They disappear as identifiable crests only near the times $t = \frac{1}{2}\pi$ and $\frac{3}{2}\pi$ of instantaneous rest.

Inspection of table 2 or of almost any of the photographs shows systematic asymmetric ($\sin nx$) modes to be present. This is, for example, clear for figure 14*c*, plate 2, in the sine coefficients and in an easily noticeable presence of the (0, 1) sloshing mode. This tendency was the most difficult to keep in bounds at the lowest depth $h' = 0{\cdot}10$ but most of the frequency measurements were made in conditions better than figure 14*c*, plate 2. Part of the reason is the single generator flap and the fact that a piston generator would have been better in shallow water. We had the definite impression, for example, for the (0, 2) modes that the purest and stablest were those for $h_*/\lambda_* = 0{\cdot}17$ probably as a result of a best fit in some sense of the flap motion to the free mode. As far as the cosine coefficients are concerned, $n = 1$ has been used to fit a_*/λ_* to the theory but the $n = 2$ and 3 coefficients show what appear to be systematic differences from the theoretical values. For the first three photos in table 2, a fair test should be possible. (Almost all the coefficients for $n = 4$ to 6 are non-significant.)

Whether or not these Fourier coefficient differences are significant and whether the extraneous harmonic content of the forced waves is having significant effects is a question of principle that affects any attempt to push these measurements as far as possible or to evaluate the degree of confidence to be placed in the ω_2 estimates. It is possible that the cosine coefficient results in table 2 are real, roughly correct, and presage differences that would be found to arise in carrying Tadjbakhsh & Keller's calculations to higher order. They could, however, also be due to failure to produce strictly free modes, the forced ones having a significantly different harmonic content and perhaps this could account for the ω_2 values differing systematically from the theoretical ones. At present, only a substantial further theoretical and experimental investigation appears capable of firmly resolving these points.

Conclusions and acknowledgments

No matter what reservations may be entered, I believe that these data conclusively confirm Tadjbakhsh & Keller's prediction of a frequency reversal in finite standing waves at approximately the depth they expect. The deviations from expectation in the ω_2 estimates and waves profiles are reasonably internally consistent and are certainly there for the experimental conditions, but whether they suggest correct conclusions for strictly free modes is certainly open to question.

This question and others mentioned earlier as to the frequency behaviour of the finite-amplitude modes as a function of amplitude would certainly appear to merit closer investigation. From the theoretical side, a calculation of the forced modes along the lines of Lin & Howard (1960) or Ursell, Dean & Yu (1960) to at least one higher order than Tadjbakhsh & Keller's series would be needed. One would also probably need to pay some attention to viscous and surface tension effects as have Keulegan (1959) and Case & Parkinson (1957) in order to interpret experimental results to the necessary precision. From the experimental side, it would be somewhat difficult but perfectly feasible to push the measurement of mode frequencies to 10^{-4} accuracy with careful choice of the generating mechanism. It would then be quite feasible to photograph wave profiles, determine a_* and the space Fourier coefficients, and determine the time behaviour of the lowest harmonics with sufficient accuracy to form a critical test of the series solutions for the wave profiles. If continuous height measurements in time were made at several points, the Fourier spectrum in time could be determined with high accuracy and conclusions concerning the space spectrum drawn.

It would also be illuminating to have a clear physical and/or formal model for the source of the frequency-effect difference between progressive and standing waves. Should one expect similar results for most types of non-linear wave motions of a gravitational character that are met with in geophysical contexts?

I have already indicated in an earlier section the manner of origin of the work reported here. I should like to repeat an acknowledgment of many discussions with Prof. G. W. Platzman, of the stimulation and questions provided by the students in the courses mentioned earlier, and of assistance and discussions with R. E. Kaylor in the design and arrangement of the apparatus and class experiments. T. S. Murty has carried out with great care most of the frequency-amplitude determinations and the detailed calculations. S. Nawrot has kept the apparatus in operating shape, Mrs Della Friedlander has done the drafting, and G. W. Gray and P. Gardiner the photographic prints.

REFERENCES

CASE, K. M. & PARKINSON, W. C. 1957 Damping of surface waves in an incompressible liquid. *J. Fluid Mech.* **2**, 172–84.

COOPER, R. M. 1960 Dynamics of liquids in moving containers. *Amer. Rocket Soc. J.* **30**, 725–9.

FOREL, F. A. 1876 La formule des seiches. *Arch. Sci. Phys. Natur. Geneve,* **57**, 278–92.

GUTHRIE, F. 1875 On stationary liquid waves. *Phil. Mag.* (4), **50**, 290–302, 377–88.

HONDA, K. & MATSUSHITA, T. 1913 An investigation of the oscillations of tank-water. *Sci. Rep. Tohoku Imp. Univ., Sendai* (1), **2**, 131–48.

KEULEGAN, G. H. 1959 Energy dissipation in standing waves in rectangular basins. *J. Fluid Mech.* **6**, 33–50.

KIRCHHOFF, G. & HANSEMANN, G. 1880 Versuche über stehende Schwingungen des Wassers. *Ann. Phys. Chem.* **10**, 337–47; *Gesammelte Abhandlungen,* pp. 442–54, 1882. Leipzig: J. A. Barth.

LAMB, H. 1932 *Hydrodynamics,* 6th ed., p. 364 ff. and p. 440 ff. Cambridge University Press.

LECHAT, F.-H. 1880 Des vibrations à la surface des liquides. *Ann. Chim. Phys.* (5), **19**, 289–344.

LIN, J. D. & HOWARD, L. N. 1960 Nonlinear standing waves in a rectangular tank due to forced oscillation. *Tech. Rep.* 44 *MIT Hydrodynamics Lab.*, ONR contracts Nonr–1841–12 and 1841 (65).

MERIAN, J. R. 1828 *Über die bewegung tropfbarer Flüssigkeiten in Gefässen.* Basle.

MOISEYEV, N. N. 1958 On the theory of nonlinear vibrations of a liquid of finite volume. *Prikl. Mat. Mekh.* **22**, 612–21 (in Russian).

PENNEY, W. G. & PRICE, A. T. 1952 Some gravity wave problems in the motion of perfect liquids. Part II. Finite periodic stationary gravity waves in a perfect liquid. *Phil. Trans.* A, **244**, 254–84.

RANKINE, W. J. M. 1865 Supplement to a paper on stream-lines. *Phil. Mag.* (4), **29**, 25–8.

RAYLEIGH, LORD 1876 On waves. *Phil. Mag.* (5), **1**, 257–79.

STOKES, SIR G. G. 1880 Considerations relative to the greatest height of oscillatory waves which can be propagated without change of form. *Math. Phys. Pap.* **1**, 225–8.

TADJBAKHSH, I. & KELLER, J. B. 1960 Standing surface waves of finite amplitude. *J. Fluid Mech.* **8**, 442–51.

TAYLOR, SIR G. 1953 An experimental study of standing waves. *Proc. Roy. Soc.* A, **218**, 44–59.

URSELL, F., DEAN, R. G. & YU, Y. S. 1960 Forced small-amplitude water waves: a comparison of theory and experiment. *J. Fluid Mech.* **7**, 33–52.

WHITE, P. & WATSON, W. 1905–6 Some experimental results in connection with the hydrodynamical theory of seiches. *Proc. Roy. Soc. Edinb.* **26**, 143–56.